Combined Synchronization and Power Control for Differentially-Encoded Di-Symbol Time-Division Multiuser Impulse Radio

Qi Zhang, Wei Cao, Arumugam Nallanathan, *Senior Member, IEEE*, and Hari Krishna Garg, *Senior Member, IEEE*

***Abstract*—The differentially-encoded, di-symbol time-division multiuser impulse radio (d^2TD-IR) with delay-sum autocorrelation receivers is a low complexity, high efficiency short range wireless communication technology for infrastructure networks. The d^2TD-IR system is designed with the assumption that the users are perfectly synchronized. In this letter, we propose a recursive algorithm of combined synchronization and power control. Computer simulation results show that the proposed algorithm has significant performance improvement over the algorithm, in which synchronization and power control are performed separately.**

***Index Terms*—Synchronization, power control, autocorrelation receiver (AcR), impulse radio (IR), ultra-wideband (UWB).**

I. Introduction

TRANSMITTED-reference impulse radios (including differential transmitted-reference impulse radios) with autocorrelation receiver (TR-IR/AcR) have been proposed in [1]-[12] for ultra-wideband (UWB) communications. The idea behind TR-IR/AcR is to exploit multipath diversity in slowly time-varying channels by coupling one or more data modulated pulses with one or more unmodulated reference pulses. The AcR delays the received reference pulses to perfectly align with the data modulated pulses and their product is integrated for symbol detection.

The major drawback of TR-IR/AcR lies in employing correlator templates that are corrupted by interference from other users and channel noise during demodulation. This induces performance degradation. To address this problem, a differentially-encoded, di-symbol time-division multiuser impulse radio (d^2TD-IR) with delay-sum autocorrelation receiver has been proposed in [10] for infrastructure networks. In the d^2TD-IR system, besides the TD multiple access scheme, two randomly generated time-hopping (TH) access sequences are employed to alternately encode the odd- and even-index symbols, hence the name di-symbol TD multiple access. The di-symbol system maximally suppresses multiuser interference (MUI) and channel noise at the expense of system complexity. It was shown through computer simulations that the d^2TD-IR system outperforms conventional time-hopping impulse radio (TH-IR) system [13] at high signal-to-noise ratio (SNR). Although the TH-IR system performs better at low SNR, its coherent detection is a challenging problem. The short duration of the pulse makes the time acquisition task formidable [14]. An acquisition error of 0.055 ns will reduce the output signal power of the detector by half when the pulse in Fig. 1 of [13] is adopted. Furthermore, the signal energy is dispersed into different multipath components. To fully exploit the signal energy, Rake receivers are often utilized to capture the energy of the signal and this usually results in highly sophisticated, hence impractical systems [15]-[18]. Therefore, the d^2TD-IR system is a promising low complexity alternative to the TH-IR system.

The d^2TD-IR system assumes perfect synchronization among users. It is thus imperative to design an efficient synchronization algorithm to support this operating condition. Synchronization algorithm for TR-IR has been studied in [19]. The algorithm is implemented in multiple steps. Each step refines the searching results by reducing the integration interval. After several steps, the algorithm is able to achieve the required synchronization accuracy. Based on the algorithm in [19], we propose a recursive algorithm of combined synchronization and power control for the multiuser d^2TD-IR system.

In the d^2TD-IR system, the transmitted signals from different users undergo independent fadings. Even when all the users are located near to the base station (BS) and have line-of-sight (LOS) to the BS, the received signal powers at the BS may be different. This is because from the free space propagation model [20], the signal power decays inversely proportional to the square of the distance from the user to the BS and such distances are different for different users. In this situation, power control, which ensures that each user provides almost the same signal power to the BS receiver, can maximally suppress the MUI and hence improve the system performance. Because both synchronization and power control processes require pilot symbols, it is preferable to combine the two processes. However, when two processes are combined, synchronization error will cause larger power control error and power control error will cause larger synchronization error. Error propagation between the two processes will cause system failure. In this letter, we propose a recursive algorithm which combines the two processes and prevents error propagation.

Manuscript received April 25, 2008; revised July 3, 2008 and October 9, 2008; accepted November 13, 2008. The associate editor coordinating the review of this letter and approving it for publications was C.-X. Wang.

Q. Zhang is with the Department of Integrated Electronics, Shenzhen Institute of Advanced Technology, Chinese Academy of Sciences, 518054, P. R. China (e-mail: qi.zhang@sub.siat.ac.cn).

W. Cao and H. K. Garg are with the Department of Electrical and Computer Engineering, National University of Singapore, 4 Engineering Drive 3, 117576, Singapore (e-mail: cao.wei@alumni.nus.edu.sg, eleghk@nus.edu.sg).

A. Nallanathan is with the Division of Engineering, King's College London, Strand Campus, London WC2R 2LS, United Kingdom (e-mail: arumugam.nallanathan@kcl.ac.uk).

This work was supported by the National University of Singapore under Grant R-263-000-436-123.

Digital Object Identifier 10.1109/TWC.2008.080572

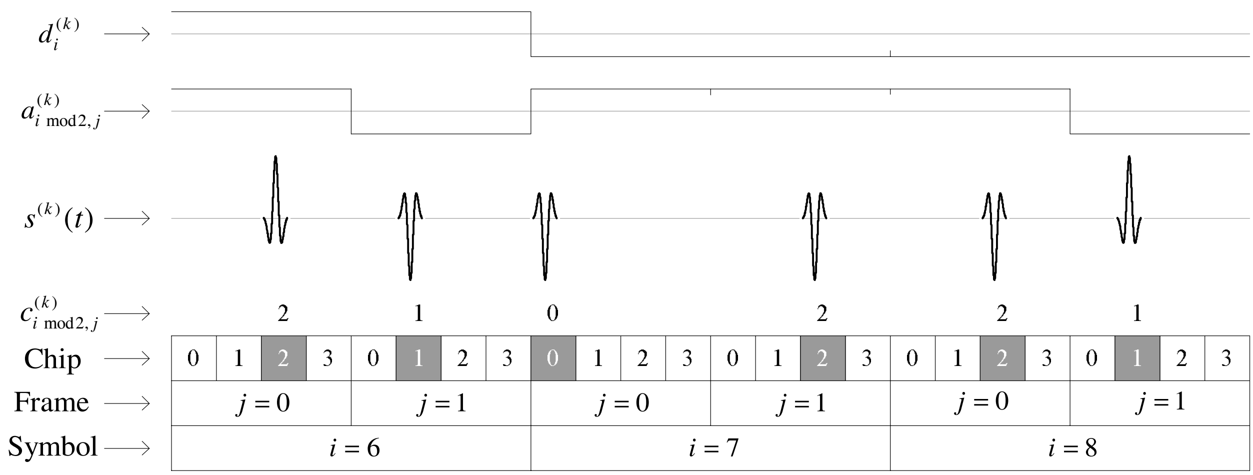

Fig. 1. Example of $s^{(k)}(t) : 6T < t \leq 9T$ for $N_h = N_u = 4$, $N_s = 2$, system with $a_{0,0}^{(k)} = 1, a_{0,1}^{(k)} = -1, a_{1,0}^{(k)} = 1, a_{1,1}^{(k)} = 1$ and $c_{0,0}^{(k)} = 2, c_{0,1}^{(k)} = 1, c_{1,0}^{(k)} = 0, c_{1,1}^{(k)} = 2$.

The rest of the letter is organized as follows. Section II describes the d^{2}TD-IR system model. In Section III, we propose a recursive algorithm which couples power control into the time of arrival (TOA) based synchronization. In Section IV, computer simulated results are presented to examine the efficiency of our proposed algorithm. We conclude and summarize our letter in Section V.

II. D^{2}TD-IR System Model

Let $\cdots b_{-1}^{(k)} b_0^{(k)} b_1^{(k)} b_2^{(k)} \cdots$ denote the sequence of independent and identically distributed (iid) information symbols sent by the k^{th} user in the N_u-user d^{2}TD-IR system, where $b_i^{(k)} \in \{-1, 1\}$. The $b_i^{(k)}$'s are first differentially encoded into another symbol sequence $\cdots d_{-1}^{(k)} d_0^{(k)} d_1^{(k)} d_2^{(k)} \cdots$, where $d_i^{(k)} = (b_i^{(k)} d_{i-1}^{(k)}) \in \{-1, 1\}$, and then transmitted using N_s non-overlapping pulses per symbol. To incorporate multiple access capability into the system, we divide each symbol interval of duration T into N_s frame intervals, further divide each frame interval into N_h chip intervals. Because TD multiple access scheme is applied here, the N_h chips are assigned to at most N_h users to transmit pulses, each user occupying one chip. The signal model for user k then has the form [10]

$$s^{(k)}(t) = \sum_i \sum_{j=0}^{N_s-1} d_i^{(k)} a_{i \bmod 2, j}^{(k)} \sqrt{\Omega^{(k)}} \, \omega\left(t - iT - jT_f - c_{i \bmod 2, j}^{(k)} T_c - T_A^{(k)}\right) \quad (1)$$

where $T_f = T/N_s$ is the frame duration, $T_c = T_f/N_h$ the chip duration, $\omega(t)$ is a causal pulse of support length $T_\omega < T_c$, $T_A^{(k)}$ is the TOA of the signals from user k and $\Omega^{(k)}$ is the power control factor of user k. In (1), the $a_{i \bmod 2, j}^{(k)}$ and $c_{i \bmod 2, j}^{(k)}$ are randomly drawn from the sets $\{-1, 1\}$ and $\{0, 1, \cdots, N_h - 1\}$, respectively, with the constraint that $c_{i \bmod 2, j}^{(k)} \neq c_{i \bmod 2, j}^{(k')} : k \neq k'$. Therefore, $[a_{0,0}^{(k)} c_{0,0}^{(k)} a_{0,1}^{(k)} c_{0,1}^{(k)} \cdots a_{0,N_s-1}^{(k)} c_{0,N_s-1}^{(k)}]$ and $[a_{1,0}^{(k)} c_{1,0}^{(k)} a_{1,1}^{(k)} c_{1,1}^{(k)} \cdots a_{1,N_s-1}^{(k)} c_{1,N_s-1}^{(k)}]$ form the multiple access code sequences assigned to the even- and odd-index symbols of user k. Alternating the two code sequences in this manner randomizes the channel-induced interference experienced by any two adjacent symbols, which in turn improves the average performance of the delay-sum AcR. An example of the structure of $s^{(k)}(t)$ is shown in Fig. 1. In the analysis to follow, we consider the full load situation where $N_h = N_u$.

The received signal due to user k is thus given by

$$r^{(k)}(t) = \sum_i \sum_{j=0}^{N_s-1} d_i^{(k)} a_{i \bmod 2, j}^{(k)} \, h^{(k)}\left(t - iT - jT_f - c_{i \bmod 2, j}^{(k)} T_c - T_A^{(k)}\right) \quad (2)$$

where

$$h^{(k)}(t) = \sum_{l=1}^{L^{(k)}} \alpha_l^{(k)} \omega(t - \tau_l^{(k)}) \quad (3)$$

is composed of $L^{(k)}$ multipath components arriving at the receive antenna with associated amplitude $\alpha_l^{(k)}$ and delay $\tau_l^{(k)}$. With perfect synchronization, $T_A^{(k)} = \tau_1^{(k)}$. The composite received signal then has the form

$$r(t) = \sum_{k=1}^{N_u} r^{(k)}(t) + n(t) \quad (4)$$

where $n(t)$ is lowpass filtered additive white Gaussian noise (AWGN) with two-sided power spectral density $N_o/2$. The autocorrelation function of $n(t)$ is

$$R_n(\tau) = \mathrm{E}[n(t)n(t+\tau)] = N_o W \mathrm{sinc}(W\tau) \quad (5)$$

where W ($W \gg 1/T_c$) is the bandwidth of the low-pass filter. The ratio E_b/N_o of the system is defined as $\frac{N_s}{N_o N_u} \int_0^{T_\omega} \omega^2(t) dt \sum_{k=1}^{N_u} \Omega^{(k)}$.

Assuming that the receiver is locked on to the signal from user k, the delay-sum AcR implements [10]

$$D_i^{(k)} : \begin{cases} > 0; \ \text{decide } b_i^{(k)} = +1 \\ \leq 0; \ \text{decide } b_i^{(k)} = -1 \end{cases} \quad (6)$$

where the decision statistics $D_i^{(k)}$ is given by

$$D_i^{(k)} = \int_{(i+1)T-T_c}^{(i+1)T} x_{i \bmod 2}^{(k)}(t) x_{(i-1) \bmod 2}^{(k)}(t-T)dt, \quad (7)$$

in which

$$x_{i \bmod 2}^{(k)}(t) = \sum_{j=0}^{N_s-1} a_{i \bmod 2,j}^{(k)} r\Big(t-(N_s-1-j)T_f \\ -(N_u-1-c_{i \bmod 2,j}^{(k)})T_c\Big). (8)$$

The underlying mechanism of (7), with (8), can be briefly explained as follows. Each of the N_s frames, indexed by $(j = 0, 1, \cdots, N_s - 1)$, of the received i^{th} symbol is first multiplied with the respective $a_{i \bmod 2,j}^{(k)}$, and then delayed based on $c_{i \bmod 2,j}^{(k)}$ so that their pulse-carrying chips are aligned. The aligned pulse-carrying chips are summed up to form a composite chip. This is then aligned and multiplied with the composite chip of the previously received $(i-1)^{th}$ symbol, and the product is integrated over one chip duration to generate the value of $D_i^{(k)}$.

III. Synchronization and Power Control for D^{2}TD-IR Systems

Before synchronization, the BS has no TOA information of the signals from different users, $\left\{T_A^{(k)}; k = 1, 2, \cdots, N_u\right\}$. In an indoor environment, the distance between the transmitter and receiver is considered to be less than 20 meters. Accordingly, the TOA is less than $20/(3 \times 10^8) = 66.67 \times 10^{-9}$ s $= 66.67$ ns, which is usually less than a frame duration. Therefore, without loss of generality, we assume that $T_A^{(\cdot)}$ is uniformly distributed over $(0, T_f]$, which denotes the initial uncertainty region U_0.

During the synchronization process, a user starts to transmit pilot symbols on receiving a cue signal from the downlink control/broadcast channel, with the assumption $T_A^{(k)} = 0$ for $k = 1, 2, \cdots, N_u$ in (1). From the composite received signal, $r(t)$, which is defined in (4) carrying only the pilot symbols, the BS estimates the TOAs of different users. With the knowledge of TOAs, the BS reschedules the transmitting time for different users. The users adjust the transmitting time based on the feedback from BS. Once synchronization process is complete, the user transmits data in the preassigned chips.

For d^{2}TD-IR systems, we will provide computer simulation results in Fig. 2 and Fig. 3 to show that power control can dramatically reduce the MUI and hence improve the system bit-error-rate (BER) performance. In this letter, perfect power control is defined as the case when the BS receives signals of equal power from different users, namely,

$$\Omega^{(k_1)} \int_0^{T_c} \left(h^{(k_1)}(t)\right)^2 dt = \Omega^{(k_2)} \int_0^{T_c} \left(h^{(k_2)}(t)\right)^2 dt \quad (9)$$

for $k_1, k_2 \in \{1, 2, \cdots, N_u\}$, where $h^{(k)}(t)$ is defined in (3). Therefore, perfect power control is achieved by finding $\Omega^{(k_1)} \neq \Omega^{(k_2)}$, for $k_1, k_2 \in \{1, 2, \cdots, N_u\}$ that satisfy (9) since $h^{(k_1)}(t) \neq h^{(k_2)}(t)$.

In this letter, we provide an approach which combines synchronization and power control based on the synchronization algorithm in [19]. Similar to [19], our synchronization approach is implemented in multiple steps. Each step aims at narrowing down the uncertainty region. We also consider to couple power control into synchronization, namely, we do power control after each step of synchronization. However, combining synchronization and power control also combines their errors, causing error propagation. The error propagation means that when the received signal power from a user is strong enough, the synchronization error will cause the estimated received signal power to be lower than the actual one, hence the user will be erroneously allocated higher transmission power. To prevent error propagation, the proposed algorithm is performed recursively as follows:

Step 1. This step performs a frame-level search. We integrate the output of the i^{th} symbol to obtain the decision statistics by using

$$D_{i,\varsigma_q}^{(k)} = \int_{(i+1)T-T_c+\varsigma_q}^{(i+1)T+\varsigma_q} x_{i \bmod 2}^{(k)}(t) x_{(i-1) \bmod 2}^{(k)}(t-T)dt \quad (10)$$

where $x_{i \bmod 2}^{(k)}(t)$ is defined in (8) and ς_q is the integration starting point in Step q. For Step 1, $\varsigma_1 = 0, T_c, 2T_c, \cdots, T_f$. The coarse TOA estimation, $\widehat{T}_{A,1}^{(k)}$, for the k^{th} user, is obtained by [19]

$$\widehat{T}_{A,1}^{(k)} = \arg\max_{\varsigma_1} \left\{ \sum_{v=\varsigma_1} D_{i,v}^{(k)} b_i^{(k)} \right\}. \quad (11)$$

In (11), the decision statistics, $D_{i,\varsigma_1}^{(k)}$, is multiplied with the pilot symbol, $b_i^{(k)}$, to get the estimation of desired signal power when the integration starting point is ς_1. For each value of ς_1, the product $D_{i,\varsigma_1}^{(k)} b_i^{(k)}$ is computed for P consecutive symbol intervals and then averaged to produce an estimate of the TOA. Averaging is required for synchronization accuracy since $D_{i,\varsigma_1}^{(k)}$ contains MUI and channel noise. Because there are $N_u + 1$ different values of ς_1, altogether $P(N_u + 1)$ pilot symbols are needed for Step 1. After the coarse TOA estimation, $\widehat{T}_{A,1}^{(k)}$, is obtained. The BS arranges the transmitted signal of the k^{th} user to be

$$s_2^{(k)}(t) = s_1^{(k)}(t - \widehat{T}_{A,1}^{(k)}) \quad (12)$$

where $s_1^{(k)}(t)$ and $s_2^{(k)}(t)$ denote the transmitted signals before and after coarse synchronization, respectively. Therefore, the uncertainty region after Step 1 is $U_1 = (-T_c, T_c]$.

The power control process is omitted in this step, since the synchronization error after this step is relatively large.

Step q ($q \geq 2$). Denote the width of uncertainty region U_{q-1} as Δ_{q-1}. The aim of this step is to reduce Δ_{q-1} to Δ_{q-1}/N, where N is an integer constant larger than one. The sampled output of the i^{th} symbol is obtained using (10), where the integration starting points are $\varsigma_q = -(N-1)\Delta_{q-1}/(2N), -(N-2)\Delta_{q-1}/(2N), \cdots, (N-1)\Delta_{q-1}/(2N)$. As in Step 1, we collect P products of $D_{i,\varsigma_1}^{(k)} b_i^{(k)}$ for each value of ς_q. Since there are $N+1$ different values of ς_q, altogether $P(N+1)$ pilot symbols are needed for Step q. The TOA estimation, $\widehat{T}_{A,q}^{(k)}$, of Step q for the k^{th} user is obtained by

$$\widehat{T}_{A,q}^{(k)} = \widehat{T}_{A,q-1}^{(k)} + \arg\max_{\varsigma_q} \left\{ \sum_{v=\varsigma_q} D_{i,v}^{(k)} b_i^{(k)} \right\}. \quad (13)$$

After TOA estimation of Step q, power control process can be performed based on $\widehat{T}_{A,q}^{(k)}$. To achieve the perfect power control condition, (9), we are required to know the estimate of

$$\int_{\widehat{T}_{A,q}^{(k)}}^{T_c+\widehat{T}_{A,q}^{(k)}} \left(h^{(k)}(t)\right)^2 dt,$$

which is denoted as $\Gamma_q^{(k)}$. The value, $\Gamma_q^{(k)}$, can be obtained as follows

$$\Gamma_q^{(k)} = \frac{1}{PN_s^2} \max\left\{\sum_{v=\varsigma_q} D_{i,v}^{(k)} b_i^{(k)}\right\}. \quad (14)$$

From [10], we know that $D_{i,v}^{(k)}$ is composed of the desired signal, the MUI and channel noise. When $N_s \gg 1$, the MUI and channel noise are approximately Gaussian with zero mean. By applying (10) and [eqn. 18-22, 10], we have

$$\mathrm{E}_\eta\left[\Gamma_q^{(k)}\right] = \int_{\widehat{T}_{A,q}^{(k)}}^{T_c+\widehat{T}_{A,q}^{(k)}} \left(h^{(k)}(t)\right)^2 dt \quad (15)$$

where η represents the pilot symbols $\{d_i^{(k)}; k = 1, 2, 3, \cdots, N_u\}$.

Before the power control process, it is required to check whether the following three conditions are satisfied to prevent error propagation. If any one of the conditions is not satisfied, we repeat Step $q-1$ with the next P incoming pilot symbols using the estimated TOAs, power control factors, and U_{q-2} obtained in Step $q-2$. These three conditions are:

1. the value $\Gamma_q^{(k)}$ for the k^{th} user is larger than zero. Since $\Gamma_q^{(k)}$ is an estimate of

$$\int_{\widehat{T}_{A,q}^{(k)}}^{T_c+\widehat{T}_{A,q}^{(k)}} \left(h^{(k)}(t)\right)^2 dt$$

which is positive, $\Gamma_q^{(k)}$ should also be positive. If not, it is due to either synchronization errors or MUI and channel noise. Because it is difficult to know which one is the actual reason, we are required to repeat Step $q-1$;

2. the minimum of $\left\{\Gamma_q^{(k)}; k = 1, 2, 3, \cdots, N_u\right\}$ in Step q is larger than that in Step $q-1$, namely,

$$\min\left\{\Gamma_q^{(k)}\right\} > \min\left\{\Gamma_{q-1}^{(k)}\right\}. \quad (16)$$

This is because the goal of power control is that the BS receives signals of equal power from different users. The k^{th} user which has the minimum of $\left\{\Gamma_{q-1}^{(k)}\right\}$ in Step $q-1$ should has been allocated more transmission power in Step q and hence should have larger $\Gamma_q^{(k)}$. If it is not the case, it proves that either error propagation exists or $\Gamma_q^{(k)}$ is corrupted by MUI and channel noise;

3. the sum of received signal power to transmitted signal power ratios of all the users in Step q is larger than that in Step $q-1$. This condition is equivalent to the inequality shown below

$$\sum_{k=1}^{N_u} \frac{\Gamma_q^{(k)}}{\Omega_q^{(k)}} > \sum_{k=1}^{N_u} \frac{\Gamma_{q-1}^{(k)}}{\Omega_{q-1}^{(k)}} \quad (17)$$

where $\Omega_q^{(k)}$ is the power control factor in Step q. Because no power control process before Step 1 and Step 2, $\Omega_1^{(k)}$ and $\Omega_2^{(k)}$ are set to be one for $k \in \{1, 2, \cdots, N_u\}$. In each step, with the shrink of uncertainty region, we should approach the actual TOAs. Therefore, if the transmission power is the same, the received signal power in Step q should be larger than that in Step $q-1$. Since the transmission power of each user is under power control, we propose to employ the ratio of the received signal power to the transmission power to evaluate whether the combined synchronization and power control process is accurate or not.

If all the conditions above are satisfied, the BS arranges the transmitted signal of the k^{th} user to be

$$s_{q+1}^{(k)}(t) = \sqrt{\Omega_{q+1}^{(k)}}\, s_q^{(k)}(t - \widehat{T}_{A,q}^{(k)}) \quad (18)$$

and proceed to do Step $q+1$. In (18), $s_q^{(k)}(t)$ and $s_{q+1}^{(k)}(t)$ denote the transmitted signals before and after Step q, respectively. To make sure that average transmission power of all the users with and without power control remains the same, we have

$$\frac{1}{N_u}\sum_{k=1}^{N_u} \Omega_q^{(k)} = 1. \quad (19)$$

Therefore, the power control factor $\Omega_{q+1}^{(k)}$ in (18) is obtained by

$$\Omega_{q+1}^{(k)} = \begin{cases} 1; & q < 2 \\ \left[\dfrac{1}{N_u}\left(\prod_{v=2}^{q}\Gamma_v^{(k)}\right)\sum_{k=1}^{N_u}\dfrac{1}{\prod_{v=2}^{q}\Gamma_v^{(k)}}\right]^{-1}; & q \geq 2. \end{cases} \quad (20)$$

The reason that $\prod_{v=2}^{q}\Gamma_v^{(k)}$ instead of only $\Gamma_q^{(k)}$ is used to compute $\Omega_q^{(k)}$ is because the transmission power of $s_q^{(k)}(t)$ is power controlled by the factor $\Omega_{q-1}^{(k)}$, which is computed based on the information of $\Gamma_2^{(k)}, \Gamma_3^{(k)}, \cdots$, and $\Gamma_{q-1}^{(k)}$.

The algorithm will stop when the width of uncertainty region is less than or equal to certain value, Δ, which is denoted as synchronization accuracy.

IV. Simulation Results

In this section, we present computer simulation results to validate our designs. As in [13], we select the shape of the pulse $\omega(t)$ to be the second derivative of a Gaussian pulse, namely, $\left[1 - 4\pi(t/\tau_m)^2\right]\exp[-2\pi(t/\tau_m)^2]$, where $\tau_m = 0.2877$ ns. The signal sampling interval is 0.167 ns. The bandwidth of the lowpass filter is 2.994 GHz. In all cases, the random channels are generated according to [21].

In Fig. 2 and Fig. 3, we compare the BER performance of ten-user d^2TD-IR system with only perfect synchronization (denoted as "PS" in the legend) and with perfect synchronization and power control (denoted as "PSPC") in CM 1 and CM 4 UWB channels [21]. The system parameters are $T_c = 10.688$ ns, $N_s = 8$ for CM 1 UWB channels and $T_c = 33.400$ ns, $N_s = 8$ for CM 4 UWB channels, respectively. From Fig. 2 and Fig. 3, it is observed that with perfect power control, the error floors at high E_b/N_o reduce to below 10^{-6}. This

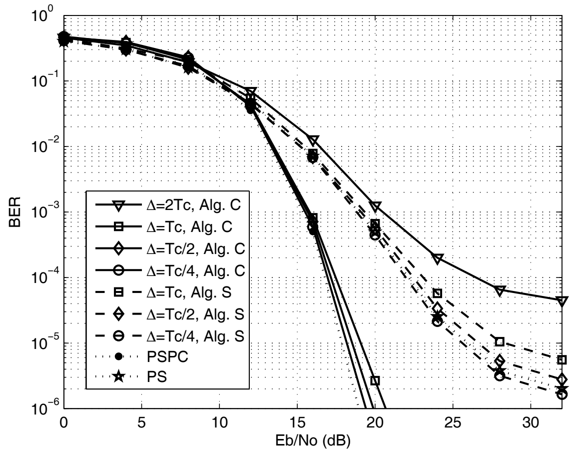

Fig. 2. BER versus E_b/N_o; comparison of ten-user d^{2}TD-IR system after combined, separated and perfect synchronization and power control in CM 1 UWB channels, where $T_c = 10.688$ ns, $N_s = 8$.

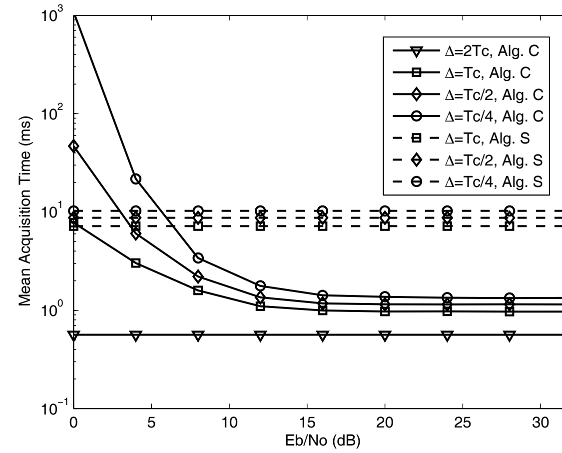

Fig. 4. MAT versus E_b/N_o; ten-user d^{2}TD-IR system after combined and separated synchronization and power control in CM 1 UWB channels, where $T_c = 10.688$ ns, $N_s = 8$.

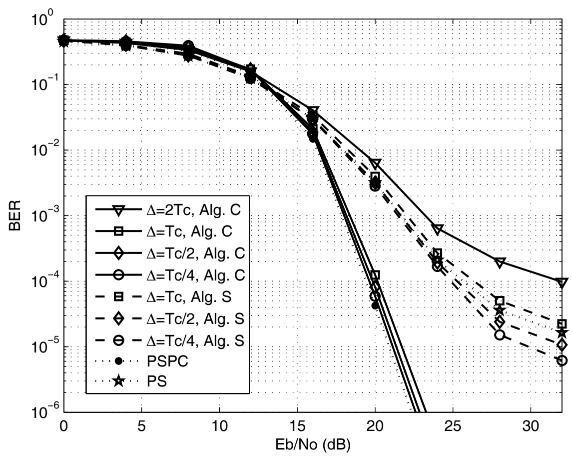

Fig. 3. BER versus E_b/N_o; comparison of ten-user d^{2}TD-IR system after combined, separated and perfect synchronization and power control in CM 4 UWB channels, where $T_c = 33.400$ ns, $N_s = 8$.

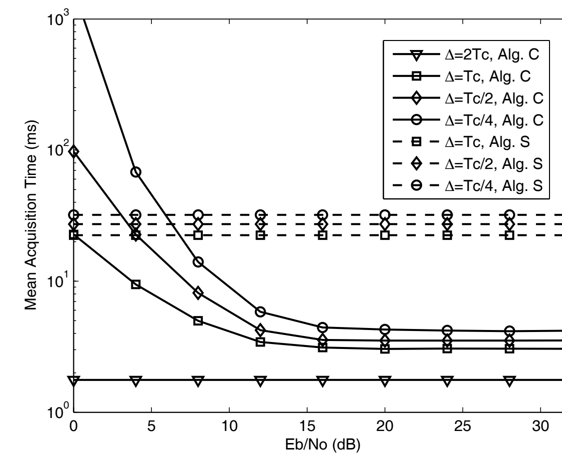

Fig. 5. MAT versus E_b/N_o; ten-user d^{2}TD-IR system after combined and separated synchronization and power control in CM 4 UWB channels, where $T_c = 33.400$ ns, $N_s = 8$.

is because the error floors are due to MUI and power control aims at reducing MUI.

In Fig. 2 and Fig. 3, we also compare the system BER performance after the recursive algorithm of combined synchronization and power control (Alg. C) with that after separated synchronization and power control (Alg. S), which means the process after (13) in Step q is not fulfilled until the synchronization is accomplished. In each step of synchronization process, the width of uncertainty regions are reduced by half ($N = 2$). Therefore, to achieve different synchronization accuracy where $\Delta = 2T_c,\ T_c,\ T_c/2,$ and $T_c/4$, it is required to perform 1, 2, 3, and 4 steps of Alg. C and Alg. S, respectively. In synchronization and power control, the number of pilot symbols for the two algorithms is related with the parameter P. We select $P = 60$ for Alg. C and $P = 600$ for Alg. S, respectively. From Fig. 2 and Fig. 3, it is observed that the system employing Alg. C performs slightly worse than that employing Alg. S when E_b/N_o is low. This is because at above situation, error propagation is severe and our proposed Alg. C may fail. However, at such low E_b/N_o, both algorithms only achieve a BER of $0.5 \sim 7\times10^{-2}$, which is not applicable for most communication systems. When E_b/N_o is high, the system employing Alg. C performs much better than that employing Alg. S. It is also found that BER performance of the system employing Alg. C when $\Delta = T_c/4$ gets very close to that under perfect synchronization and power control.

Compared with non-recursive Alg. S, the recursive Alg. C has a property that the acquisition time is not deterministic. To examine the efficiency of our proposed algorithm, we compute the mean acquisition time (MAT) for the d^{2}TD-IR system. In this letter, the MAT is defined as the average time duration, or (average number of pilot symbols) $\times$ (symbol duration), to achieve the required synchronization accuracy over different channel realizations. The MAT at various E_b/N_o for the simulations in CM 1 and CM4 UWB channels are plotted in Fig. 4 and Fig. 5, respectively. It is noticed that the MAT remains the same for Alg. S and it reduces exponentially with the increase of E_b/N_o for Alg. C when $\Delta = T_c,\ T_c/2,$ and $T_c/4$. When

$E_b/N_o > 14$ dB, the BER and MAT performance curves show that Alg. C outperforms Alg. S. At E_b/N_o of 24 dB, to achieve $\Delta = T_c/4$ only requires MAT of about 1.37 ms (or about 1602 pilot symbols) on average for Alg. C in CM 1 UWB channels and about 4.30 ms (or about 1608 pilot symbols) in CM 4 UWB channels, respectively.

V. Conclusions

In this letter, we have proposed a recursive algorithm of combined synchronization and power control for the d^{2}TD-IR system. The computer simulation results have shown that when $\Delta = T_c/4$, the proposed algorithm is capable of achieving similar performance of the system under perfect synchronization and perfect power control. It is also found that the proposed algorithm is much more efficient than the algorithm, in which synchronization and power control are performed separately.

References

[1] R. T. Hoctor and H. W. Tomlinson, "Delay-hopped transmitted-reference RF communications," in *Proc. UWBST 2002*, pp. 289-292.

[2] M. Ho, V. S. Somayazulu, J. Foerster, and S. Roy, "A differential detector for an ultra-wideband communications system," in *Proc. VTC 2002-Spring*, pp. 1896-1900.

[3] J. D. Choi and W. E. Stark, "Performance of ultra-wideband communications with suboptimal receivers in multipath channels," *IEEE J. Select. Areas Commun.*, vol. 20, pp. 1754-1766, Dec. 2002.

[4] T. Q. S. Quek, M. Z. Win, and D. Dardari, "UWB transmitted reference signaling schemes–part I: performance analysis," in *Proc. ICU 2005*, pp. 587-592.

[5] T. Q. S. Quek and M. Z. Win, "Analysis of UWB transmitted-reference communication systems in dense multipath channels," *IEEE J. Select. Areas Commun.*, vol. 23, pp. 1863-1874, Sept. 2005.

[6] F. Tufvesson and A. F. Molish, "Ultra-wideband communication using hybrid matched filter correlation receivers," in *Proc. VTC 2004-Spring*, pp. 1290-1294.

[7] L. Yang and G. B. Giannakis, "Optimal pilot waveform assisted modulation for ultrawideband communications," *IEEE Trans. Wireless Commun.*, vol. 3, pp. 1236-1249, July 2004.

[8] A. A. D'Amico and U. Mengali, "GLRT receivers for UWB systems," *IEEE Commun. Lett.*, vol. 9, pp. 487-489, June 2005.

[9] K. Witrisal, G. Leus, M. Pausini, and C. Krall, "Equivalent system model and equalization of differential impulse radio UWB systems," *IEEE J. Select. Areas Commun.*, vol. 23, pp. 1851-1862, Sept. 2005.

[10] Q. Zhang and C. S. Ng, "Differentially-encoded di-symbol time-division multiuser impulse radio in UWB channel," *IEEE Trans. Commun.*, vol. 56, pp. 608-618, Apr. 2008.

[11] Q. Zhang and C. S. Ng, "DSTBC impulse radios with autocorrelation receiver in ISI-free UWB channels," *IEEE Trans. Wireless Commun.*, vol. 7, pp. 806-811, Mar. 2008.

[12] D. L. Goeckel and Q. Zhang, "Slightly frequency-shifted reference ultra-wideband (UWB) radio," *IEEE Trans. Commun.*, vol. 55, pp. 508-519, Mar. 2007.

[13] M. Z. Win and R. A. Scholtz, "Ultra-wide bandwidth time-hopping spread-spectrum impulse radio for wireless multiple-access communications," *IEEE Trans. Commun.*, vol. 48, pp. 679-691, Apr. 2000.

[14] W. Suwansantisuk, M. Z. Win, and L. A. Shepp, "On the performance of wide-bandwidth signal acquisition in dense multipath channels," *IEEE Trans. Veh. Technol.*, vol. 54, pp. 1584-1594, Sept. 2005.

[15] V. Lottici, A. D'Andrea, and U. Mengali, "Channel estimation for ultra-wideband communications," *IEEE J. Select. Areas Commun.*, vol. 20, pp. 1638-1645, Dec. 2002.

[16] M. Z. Win and R. A. Scholtz, "On the robustness of ultra-wide bandwidth signals in dense multipath environments," *IEEE Commum. Lett.*, vol. 2, pp. 51-53, Feb. 1998.

[17] M. Z. Win and Z. A. Kostic, "Virtual path analysis of selective Rake receiver in dense multipath channels," *IEEE Commun. Lett.*, vol. 3, pp. 308-310, Nov. 1999.

[18] M. Z. Win, G. Chrisikos, and N. R. Sollenberger, "Performance of Rake reception in dense multipath channels: implications of spreading bandwidth and selection diversity order," *IEEE J. Select. Areas Commun.*, vol. 18, pp. 1516-1525, Aug. 2000.

[19] N. He and C. Tepedelenlioglu, "Adaptive synchronization for non-cohenrent UWB receivers," in *Proc. ICASSP 2004*, pp. 517-520.

[20] T. S. Rappaport, *Wireless Communications: Principles and Practice*. New Jersey: Prentice Hall, 1996.

[21] J. Foerster, *et al.*, "Channel Modeling Sub-committee Report Final," IEEE802.15-02/490, Nov. 2003.